

PAPER • OPEN ACCESS

## CFD-based casing and distributor hydraulic design optimization

To cite this article: C Devals *et al* 2019 *IOP Conf. Ser.: Earth Environ. Sci.* **240** 022033

View the [article online](#) for updates and enhancements.

You may also like

- [Natural growth and development stimulants of Lucerne plants](#)  
S A Bekuzarova, A T Farniev, A Kh Kozyrev et al.
- [Thermoneutral Operation of Solid Oxide Electrolysis Cells in Potentiostatic Mode](#)  
Ming Chen, Xiufu Sun, Christodoulos Chatzichristodoulou et al.
- [Reducing the risk of hallucinations with interpretable deep learning models for low-dose CT denoising: comparative performance analysis](#)  
Mayank Patwari, Ralf Gutjahr, Roy Marcus et al.



**ECS**  
The  
Electrochemical  
Society  
Advancing solid state &  
electrochemical science & technology

**DISCOVER**  
how sustainability  
intersects with  
electrochemistry & solid  
state science research

# CFD-based casing and distributor hydraulic design optimization

C Devals<sup>1</sup>, N Murry<sup>2</sup>, B F Mullins<sup>2</sup>, J Dompierre<sup>1</sup>, L Mangani<sup>3</sup> and F Guibault<sup>1</sup>

<sup>1</sup> École Polytechnique de Montréal, Montréal, QC, Canada

<sup>2</sup> Andritz Hydro, Pointe-Claire, QC, Canada

<sup>3</sup> Lucerne University of Applied Sciences and Arts, Technik & Architektur, Horw, Switzerland

E-mail: christophe.devals@polymtl.ca

**Abstract.** With recent advances in computational power, it is possible to optimize the design of complex hydraulic components such as casings and distributors in addition to runners and draft tubes. Continuing our previous work on CFD-based draft tube hydraulic design optimization, we present a procedure based on a metamodel-assisted evolutionary optimization algorithm comprising a parametric casing and distributor hydraulic geometry model and a hydraulic efficiency evaluation using an in-house mesh generator and a coupled finite volume flow solver developed by the University of Lucerne (HSLU). The approach can take hydraulic performance as well as mechanical stresses and civil engineering constraints into account, with the goal of helping designers obtain better overall solutions than with traditional design methods alone.

## 1. Introduction

Designing hydraulic components for a new project or to rehabilitate an existing one is not an easy task. Optimization can help accelerate the design process and improve the performance of all components by exploring a design space in a more efficient and systematic way. Examples of draft tube, Francis runner, Kaplan runner, and radial pump impeller optimizations can be found in [1-4]. Alnaga and Kueny [5] present an automatic iterative procedure for optimal design of hydraulic turbine distributors using evolutionary algorithms. In [6], a single objective optimization for stay vanes and a multi-objective optimization for runners were carried out. With the recent advances in computational power, it is now possible to optimize the design of complex hydraulic components such as casings and distributors *at the same time*, which, does not seem to have been reported in the literature so far.

To achieve this goal and in continuation of previous work done on CFD-based draft tube design optimization, several topics must be addressed: parametric CAD and automatic mesh generation [7], mesh validation [8], assessment of the influence of mesh properties on solution quality, computational fluid dynamics (CFD) validation [9-11], tool automation, optimization methodology including choice of search algorithm, parametric design model and cost function [1-2].

## 2. Parametric design

Casing and distributor geometries can be very complex and design models often involve hundreds of parameters. While it is possible to optimize a problem containing several hundred parameters, due to the time required to evaluate the performance of a single casing and distributor design, such a large optimization is impractical in a turbine development context. Therefore, a simplified parametric model



was developed that is capable of reproducing the most important features of modern casing and distributor designs, but with significantly fewer variables. The parametric model consists of several sub-components and provides the ability to parameterize and thus optimize specific parts of the geometry while leaving the remaining parts unchanged. This flexibility can be useful in rehabilitation projects where the casing and stay ring geometry is usually fixed, but where the stay vanes and guide vanes may be modified or replaced.

During the course of an optimization, numerous combinations of design parameter values are generated, but not all of these combinations will result in acceptable casing and distributor designs. In addition to the obvious parameter range constraints, the functionality of the resulting geometry must be checked. Do the guide vanes close? Will the guide vanes interfere with the stay vanes and/or the runner? Does the resulting geometry meet the minimum stress requirements? If the answer to any of these questions is “no”, the design is rejected and its performance not evaluated.

The following sections describe the parameterization of each sub-component in detail.

### 2.1. Spiral casing

Spiral casings are typically designed using 20 or more circular planar sections and consist of an inlet part that receives water from the penstock and a spiral part that redirects the water into the distributor. The inlet sections roughly form a straight pipe, while the spiral sections are arranged around the distributor in usually monotonically decreasing cross-section area.

The inlet part begins with a circular section whose centre is offset with respect to the machine centreline and ends with the first circular section of the spiral forming an oblique tapered cylinder. The spiral part consists of several circular control sections from which the actual sections are interpolated (figure 1).

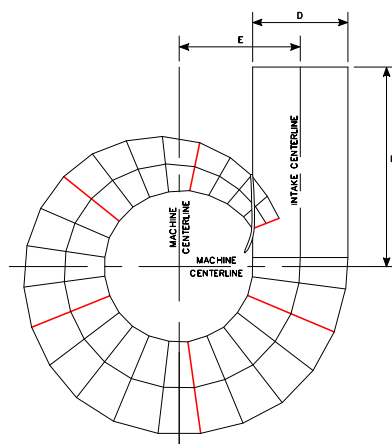


**Figure 1.** Casing parameterization.

Control sections are red and interpolated sections are black.

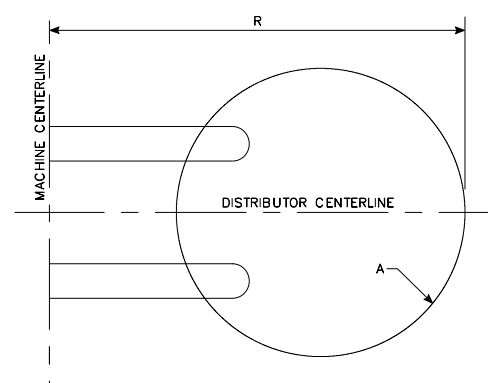


**Figure 2.** Casing control section parameterization.

A casing control section (figure 2) is defined by a cross-section area and a radial distance between the machine centreline and its outer side, and its position as a fraction of spiral length. The actual casing sections are interpolated from the control sections.

### 2.2. Distributor rings

Distributor rings (figure 3) consist of two parallel plates that form the parts of the stay ring that are attached to the casing and hold the guide vanes in place. The distributor rings are defined by an upper and lower plate thickness, an outer radius and a distance between the plates (distributor height).

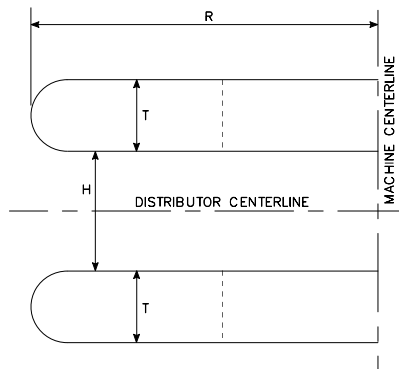


**Figure 3.** Distributor ring parameterization.

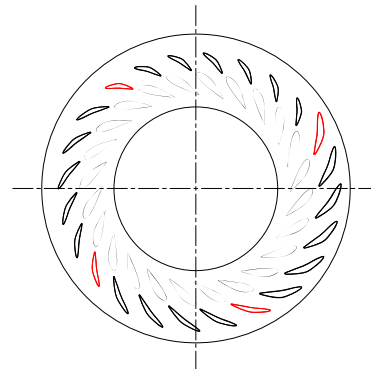


**Figure 4.** Stay vane parameterization.  
Control stay vanes are red and interpolated stay vanes are black.

### 2.3. Vane profile

The parametric model supports several vane profile parameterizations. A parameterization based on the work by Boeing Aerospace engineers, Kulfan and Bussoletti [12], is preferred due to its ability to accurately parameterize a wide variety of existing stay vane and guide vane profile geometries and to produce new and innovative profiles in the context of casing and distributor design optimization.

### 2.4. Stay vanes

Stay vanes are attached to the distributor rings and direct the water in the casing towards the guide vanes in a uniform way. Typical stay vane designs consist of 20 to 30 vanes that are usually arranged in decreasing size around the distributor. The stay vane parameterization (figure 4) consists of a base vane profile from which the actual stay vanes are interpolated via several control points that scale and reposition the base vane profile as a function of stay vane position index. The stay vane control points consist of scaling factors for length and thickness and an installation angle.

### 2.5. Guide vanes

Guide vanes are hydraulic surfaces that control the amount of water flow to the runner and therefore the output power. The guide vanes (figure 5) are defined by a vane profile, a pivot point, a pivot circle diameter and an angular position.

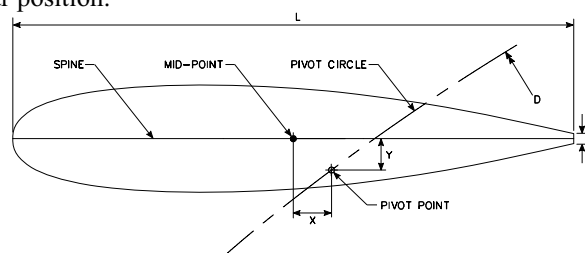


**Figure 5.** Guide vane parameterization.

## 3. Computational fluid dynamics

An in-house mesh generator and a block coupled solver, *coupledNumerics* [13], are used to compute the steady viscous flow solution by solving the Reynolds Averaged Navier-Stokes equations using the standard  $k-\epsilon$  turbulence model with wall-function.

### 3.1. Mesh generation

The geometry of the casing and distributor is exported from the in-house geometry design tool using the parametric model described above.

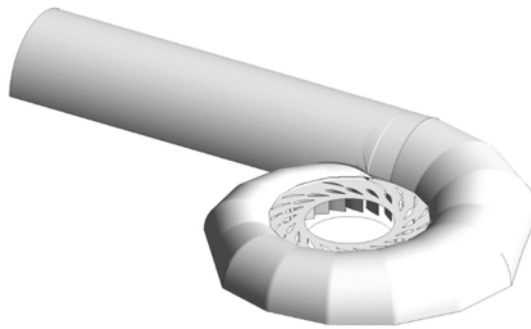


**Figure 6.** Initial casing-distributor 3D geometry.

The challenge in the meshing of such geometries lies in the ability to automatically generate casing and distributor meshes for different guide vane opening angles. In order to facilitate the meshing task, the flow domain has been divided into two sub-domains; one for the spiral casing and the other for the distributor. In-house automatic mesh generators providing hexahedral and prismatic elements are used to generate the meshes for both components. The distributor mesh has to be generated for every change in guide vane opening position while the casing mesh is generated only once. The distributor mesh contains concentrated hexahedral elements in the vicinity of the vane profiles to resolve the flow boundary layer and prismatic elements in the flow field. A description of the technology used to construct this type of hybrid meshes can be found in [7]. The spiral casing mesh contains only hexahedral elements.

Because a large number of calculations are necessary for optimization, a symmetric coarse grid is used without losing too much precision [10]. In the context of optimization, the use of a coarse mesh is acceptable since the relative performance between different designs is of primary importance and not the absolute performance for any given design. The casing mesh with 1.4M vertices and 1.3M elements and the distributor mesh with 4.0M vertices and 7.0M elements are exported in the CGNS (CFD General Notation System) format [14] and are shown in figure 7. The average dimensionless wall distance  $Y^+$  is between 17 and 22.

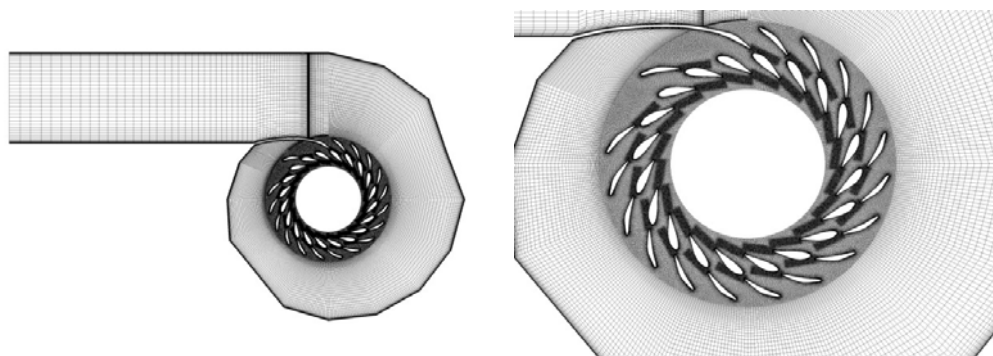


**Figure 7.** Initial mesh for casing and distributor (left) and zoom on the distributor (right).

Once the mesh has been generated, an automatic script creates all of the necessary files for the CFD setup, simulations and post-processing.

### 3.2. Block coupled solver

*coupledNumerics*, a new block coupled solver based on algorithms described by Darwish and Mangani [15-16], was used in the simulations reported in this paper. In *coupledNumerics*, the Navier-Stokes equations are discretized as one coupled system resulting in a set of block algebraic equations. These equations are then solved using an algebraic multi-grid solver, which combined with the implicit discretization, ensures that computational cost scales linearly with mesh size.

Because of the inter-variable coupling, no under-relaxation is needed in the equation; instead a transient time stepping scheme is used where the time step is generally related to the problem time scale. This combination has been demonstrated by Darwish et al. [15-16] and results in a solution time that can be 30 times smaller than segregated solvers in addition to increased robustness and less sensitivity to initial conditions. *coupledNumerics* also includes a number of high resolution schemes and turbulence models. In this work, a  $k$ - $\varepsilon$  turbulence model was used.

**3.2.1. Numerical scheme.** A second order bounded scheme was used for all simulations. The scheme uses a base second order upwind method combined with total variation diminishing (TVD) to limit any over or under shoot. The robustness of the scheme means that there is no need to start the solution using the first order upwind scheme and then switch to a higher order scheme.

**3.2.2. Boundary conditions.** For optimization, steady state calculations are performed with convergence criteria of residual values lower than 1e-6 based on the root mean square (RMS). At the inlet of the casing, a constant flow rate is imposed. At the outlet of the distributor, an average constant pressure of 0 Pa is used. Two arbitrary fully conservative mesh interfaces (Multiple Mesh Interface) are used between the intake and the casing and between the spiral casing and the distributor. At the wall, no slip velocity conditions are used. The turbulence kinetic energy  $k$  and the turbulence eddy dissipation  $\varepsilon$  are initialized with  $k_{inlet} = 3/2(V_{inlet})^2$ ,  $\varepsilon_{inlet} = C_{mu}^{0.75} k^{1.5} / L_t$  respectively, where  $I$  is the turbulence intensity,  $V_{inlet}$  is the velocity at the inlet based on the flow rate,  $C_{mu}$  is the  $k$ - $\varepsilon$  model parameter typically set to 0.09 and  $L_t$  is the turbulent mixing length.

## 4. Optimization method

A metamodel-assisted evolutionary algorithm (MAEA) was used to perform the casing and distributor design optimization. The details on this optimization method can be found in previous work on CFD-based draft tube design optimization [1].

## 5. Casing and distributor design optimization

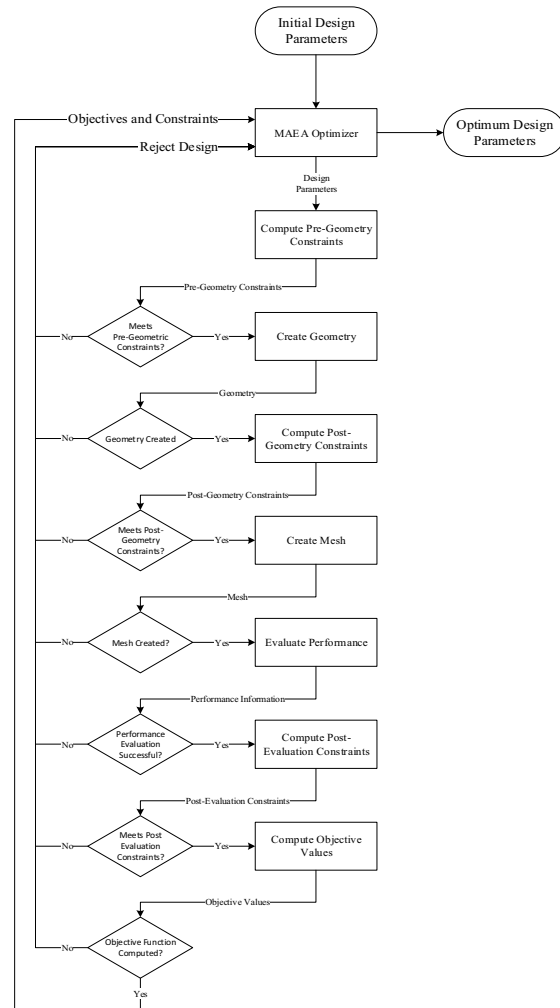
An in-house casing and distributor design optimization tool was developed and tested to determine if it was capable of producing useful results within a reasonable length of time. To this end, it was decided to first perform a simple “academic” test to ensure that the mechanics of the optimization loop (figure 8) were working, and then proceed with a more realistic test. In both cases, the population sizes used for the MAEA were  $\mu=5$  parents and  $\lambda=10$  offspring. It should be noted that the casing and distributor design in the presented example is not an Andritz Hydro design, but rather an arbitrary test case.

### 5.1. Academic optimization

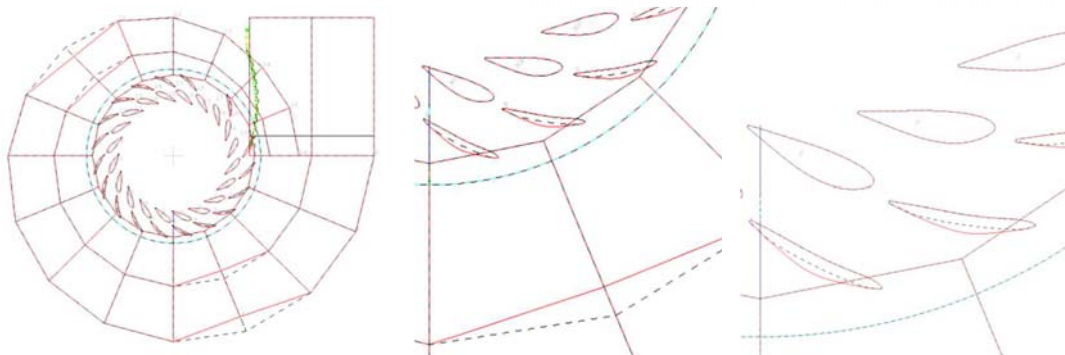
For the academic optimization, an old casing and distributor design was chosen consisting of 18 stay vanes and 20 guide vanes. The idea is to perform a small and relatively quick optimization by arbitrarily deforming the original geometry and then using it as a starting point to see if the optimizer can produce a design that is similar to the original. The original design was deformed by reducing the area of two casing sections and by increasing the profile thickness of the stay vanes as shown in figure 9.

A bi-objective optimization was performed by minimizing the total pressure difference between the inlet and the outlet of the casing and of the distributor (stay vane and guide vane) separately. The parametric model consisted of 163 parameters, of which only three were allowed to vary: the area of the two deformed casing sections and the stay vane base profile thickness. The performance was evaluated at the best efficiency operating condition for the original design, which corresponded to a guide vane opening angle of  $26^\circ$ . The outer radii of the deformed casing sections were not allowed to exceed that of the original geometry and the stay vane areas were not permitted to be less than the original design. The optimization ran for seven generations and produced a total of 67 designs before a “best” design that looked like the original design was obtained.

The total pressure was extracted in the planes as shown in figure 10 and the losses are given in table 1. Figure 11 shows a contour plot of the total losses at mid-distributor for three casing and distributor geometries designated as original, initial and best—these plots give an idea of where the losses occurred and are not necessarily indicative of overall performance.

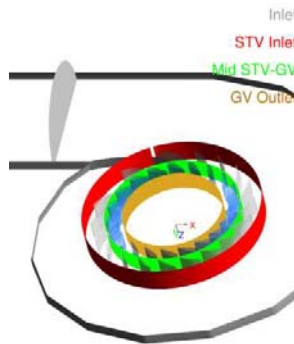


**Figure 8.** Optimization loop.

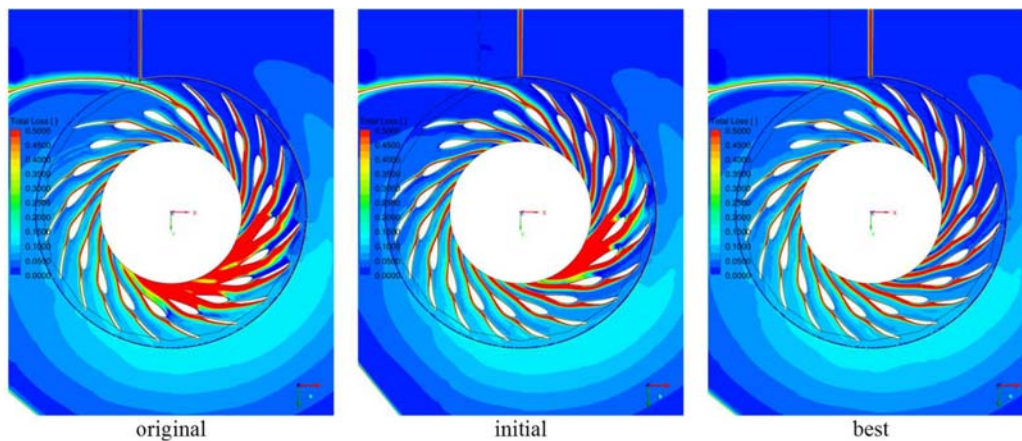


**Figure 9.** Original (dashed black line) and initial (red line) geometry.

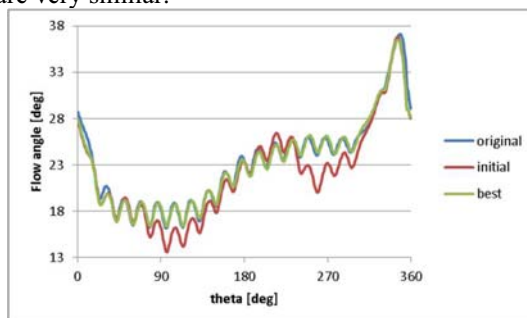
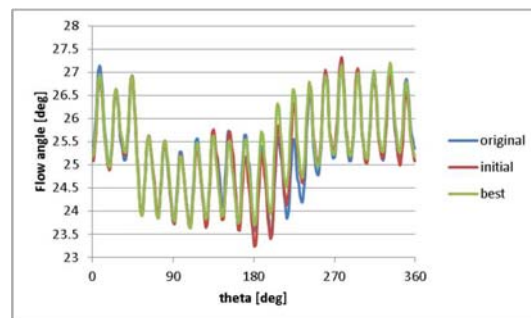


**Table 1.** Losses in  $\% \rho g H$  for unit flow condition.

	Casing	Stay Vane	Guide Vane	SV + GV	Casing + Distributor
Original	0.0148	0.2571	0.2547	0.5118	0.5266
Initial	0.0222	0.2850	0.2831	0.5681	0.5903
Best	0.0141	0.2401	0.2336	0.4737	0.4878

**Figure 10.** Loss planes.**Figure 11.** Total losses at mid-distributor.

The flow angle at the leading edge of the stay vanes and at the trailing edge of the guide vanes for the three geometries are compared in figure 12 and figure 13 respectively. Original and best geometries are very similar.

**Figure 12.** Flow angle at stay vane inlet.**Figure 13.** Flow angle at guide vane outlet.



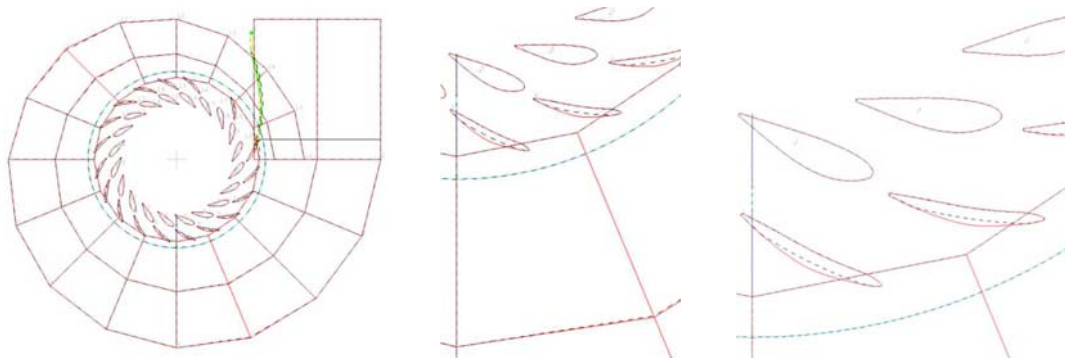


**Figure 14.** Original (dashed black line) and best (red line) geometry.

A comparison in figure 14 between the original and the best geometry found by the optimization shows that both geometries are very similar except for the stay vanes. The best stay vanes are thicker than the ones in the original design and the results, in terms of losses, are remarkably different.

### 5.2. Realistic optimization

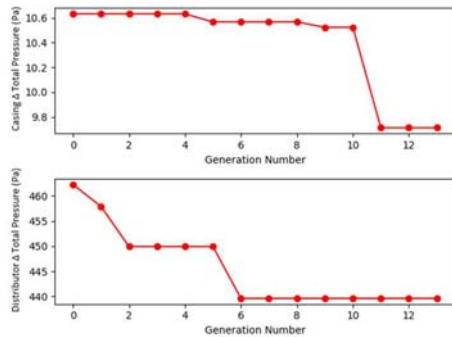
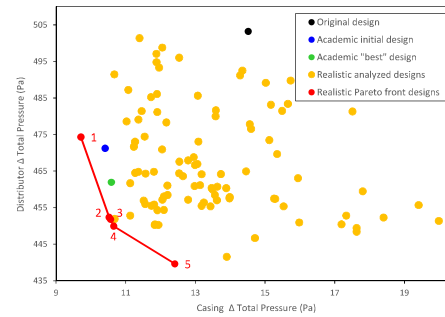
A second, more realistic test was performed with the goal of obtaining a design with significantly better performance compared to the original. As in the academic case, a bi-objective optimization was performed by independently minimizing the total pressure difference between the inlet and outlet of the casing and of the distributor. In this test, the “best” design from the previous test was used as the starting point since its performance was already better than the original. The parametric model consisted of 125 parameters, of which 85 were fixed, 25 were directly controlled by the optimizer (table 2) and 15 were derived (i.e. computed).

**Table 2.** Variable parameters.

Sub-component	Number of Parameters	Comments
Inlet	1	1 diameter, fixed length
Casing	8	4 control sections, 2 parameters per section
Stay Vane	10	5 profile parameters, 5 control orientations, base stay vane profile not scaled
Distributor Rings	0	not modified
Guide Vane	6	5 profile parameters, 1 head cover rotation angle, fixed pivot point

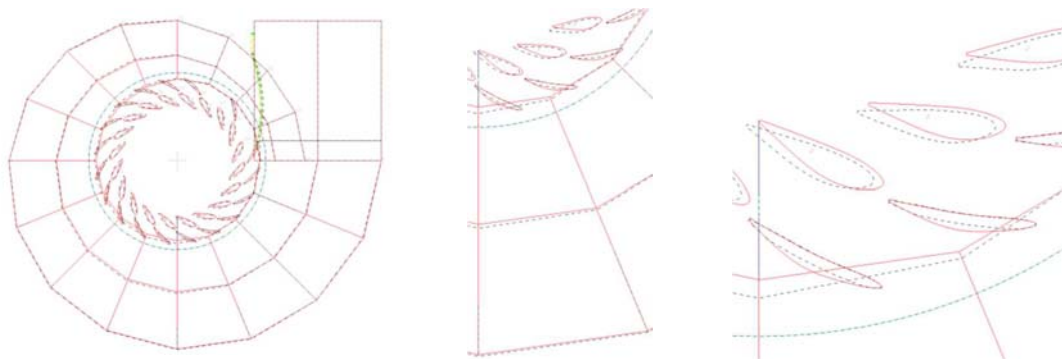
The size of the casing was constrained to not exceed the outer diameter of the original design and the stay vane and guide vane areas were constrained to be greater than or equal to the corresponding areas in the original vanes. For each design, after the performance was evaluated, the flow velocity field near the guide vane outlet was checked to ensure that it met the runner design criteria.

The optimization ran for 6 days, producing a total of 144 analyzed designs in 13 generations. Figure 15 shows how the casing and distributor objectives evolved as the optimization progressed and figure 16 shows the best designs (1 to 5) in the Pareto front of the last generation before the optimization was terminated.

**Figure 15.** Convergence plot.**Figure 16.** Pareto front.**Table 3.** Optimization Results.

Test	Design	Casing	Stay Vane	Guide Vane	Total	Casing	Stay Vane	Guide Vane	Total
		Loss % $\rho gH$ (at unit flow)				Loss % Change (Original)			
N/A	Original	0.0148	0.2571	0.2547	0.5266	0	0	0	0
Academic	Initial	0.0222	0.2850	0.2831	0.5903	50.14	10.85	11.14	12.09
	Best	0.0141	0.2401	0.2336	0.4878	-4.80	-6.60	-8.29	-7.37
Realistic	Pareto 1	0.0098	0.2389	0.2417	0.4905	-33.34	-7.05	-5.12	-6.86
	Pareto 2	0.0110	0.2343	0.2363	0.4816	-25.83	-8.85	-7.22	-8.54
	Pareto 3	0.0109	0.2320	0.2323	0.4751	-26.44	-9.76	-8.81	-9.77
	Pareto 4	0.0111	0.2331	0.2373	0.4815	-24.56	-9.34	-6.85	-8.56
	Pareto 5	0.0130	0.2421	0.2168	0.4718	-12.25	-5.84	-14.89	-10.40

Table 3 summarizes the losses for both the academic and realistic optimizations. As can be seen, the Pareto 5 design (figure 17) from the realistic optimization has the best overall performance with the remaining four designs in the Pareto front having slightly higher overall losses, but having sub-components with better or worse losses than the best overall design.

**Figure 17.** Original (dashed black line) and design Pareto 5 (red line) geometry.

## 6. Conclusion

This paper has presented a CFD-based casing and distributor optimization scheme that is suitable for use within a turbine development context. It has been shown that realistic designs using a fairly large number of design parameters can be optimized for hydraulic performance using a sophisticated 3D

viscous flow CFD approach and that this can be done within a reasonable time frame on generally available computing resources by utilizing a MAEA optimization scheme. This tool will help designers to accelerate the design process by exploring a design space more efficiently in order to improve the performance of all components. Extension of the current optimization scheme to include the runner and the draft tube will be investigated in the future.

## References

- [1] McNabb J, Devals C, Kyriacou S A, Murry N and Mullins B F 2014 CFD based draft tube hydraulic design optimization *IOP Conf. Ser.: Earth Environ. Sci.* **22** 012023
- [2] Bahrami S, Tribes C, Devals C, Vu T C and Guibault F 2016 Multi-fidelity shape optimization of hydraulic turbine runner blades using a multi-objective mesh adaptive direct search algorithm *Applied Mathematical Modeling* **40** 1650-68
- [3] Semenova A, Chirkov D, Lyutov A, Cherny S, Skorospelov V and Pylev I 2014 Multi-objective shape optimization of runner blade for Kaplan turbine *IOP Conf. Ser.: Earth Environ. Sci.* **22** 012025
- [4] Kyriacou S, Kontoleon E, Weissenberger S, Mangani L, Casartelli E, Skouteropoulou I, Gattringer M, Gehrler A and Buchmayr M 2014 Evolutionary algorithm based optimization of hydraulic machines utilizing a state-of-the-art block coupled CFD solver and parametric geometry and mesh generation tools *IOP Conf. Ser.: Earth Environ. Sci.* **22** 012024
- [5] Alnaga A and Kueny J L 2008 Optimal design of hydraulic turbine distributor *WSEAS Transaction on Fluid Mechanics* **3** 175-185
- [6] Kawajiri H, Enomoto Y and Kurosawa S 2014 Design optimization method for Francis turbine *IOP Conf. Ser.: Earth Environ. Sci.* **22** 012026
- [7] Guibault F, Zhang Y, Dompierre J and Vu T C 2006 Robust and automatic CAD-based structured mesh generation for hydraulic turbine component optimization *Proc. 23rd IAHR Symposium on Hydraulic Machinery and Systems* Yokohama Japan
- [8] Devals C, Vu T C, Zhang Y, Dompierre J and Guibault F 2016 Mesh convergence study for hydraulic turbine draft tube *IOP Conf. Ser.: Earth Environ. Sci.* **49** 082021
- [9] Vu T C, Devals C, Zhang Y, Nennemann B and Guibault F 2011 Steady and unsteady flow computation in an elbow draft tube with experimental validation *Int. J. Fluid Machinery and Systems* **4** 85-96
- [10] Devals C, Vu T C and Guibault F 2015 CFD analysis for aligned and misaligned guide vane torque prediction and validation with experimental data *Int. J. Fluid Machinery and Systems* **8** 132-141
- [11] Devals C, Zhang Y, Dompierre J, Vu T C Mangani L and Guibault F 2015 3D casing-distributor analysis for hydraulic design application *Int. J. Fluid Machinery and Systems* **8** 142-154
- [12] Kulfan B M and Bussoletti J E 2006 Fundamental parametric geometry representations for aircraft component shapes *11th AIAA/ISSMO Multidisciplinary Analysis and Optimization Conference* Portsmouth, VA, USA
- [13] coupledNumerics is developed by coupledNumerics gmbh, Luzerne, Switzerland
- [14] Available at: [http://cgns.github.io/CGNS\\_docs\\_current/sids/index.html](http://cgns.github.io/CGNS_docs_current/sids/index.html)
- [15] Darwish M, Mangani L and Moukalled F 2018 Implicit boundary conditions for coupled solvers *Computers and Fluids* **168** 54-66
- [16] Darwish M, Sraj I and Moukalled F 2009 A coupled finite volume solver for the solution of incompressible flows on unstructured grids *J. Computational Physics* **228** 180-201